Zeitschrift: Eclogae Geologicae Helvetiae
Herausgeber: Schweizerische Geologische Gesellschaft
Band: 85 (1992)
Heft: 2

Artikel: Testing a new multichannel controlled-source audio magnetotelluric method (CSAMT) on a borehole

Autor: Schnegg, Pierre-André

DOI: https://doi.org/10.5169/seals-167015

Eclogae geol. Helv. 85/2: 459–470 (1992)

0012-9402/92/020459-12 $ 1.50 + 0.20/0
Birkhäuser Verlag, Basel

Testing a new multichannel controlled-source audio magnetotelluric method (CSAMT) on a borehole

By Pierre-André Schnegg [1])

Key words: Magnetotellurics, CSAMT, Controlled-Source Audio Magnetotellurics

ABSTRACT

The controlled-source magnetotelluric method (CSAMT) has been tested on the site of a borehole where the electrical resistivity is known down to a depth of 704 m. This test was performed in order to establish, under well-controlled experimental conditions, the validity of our method, and to find its limits. The results show excellent agreement with the known electrical characteristics of the geology, both in resistivity and layer thickness determination.

RÉSUMÉ

La méthode de sondage magnétotellurique à source contrôlée (CSAMT, Controlled-Source Audio MagnetoTellurics) a été testée sur le site d'un forage pour lequel nous disposions des résultats de la mesure de la résistivité électrique jusqu'à 704 mètres de profondeur. Cette comparaison a pour but d'établir dans des conditions précises la validité de notre méthode, et d'en explorer les limites. Le résultat du sondage montre un excellent accord avec les données du forage, tant dans la détermination des résistivités que dans celle de l'épaisseur des couches géologiques.

1. Introduction

The magnetotelluric method

The sounding technique described in this paper stems from the universally used magnetotelluric (MT) method which was independently developed in the fifties both in the USSR (Tikhonov 1950) and France (Cagniard 1953).

The principles of the original one-dimensional MT method are simple: the sounding site, whose rock resistivity distribution with respect to depth is of interest, is permanently subjected to electromagnetic fields of natural (Keller & Frischknecht 1979) or man-made origin (Szarka 1987). At the Earth's surface both electric and magnetic fields are recorded simultaneously for periods of time proportional to the square of the desired investigation depth (one minute to several days). From these records, parameters directly related to the nature of the underlying rocks are derived: the MT apparent resistivity is expressed as

$$\varrho(f) = \frac{1}{5f}\left|\frac{E(f)}{H(f)}\right|^2, \qquad (1)$$

[1]) Observatoire Cantonal, CH-2000 Neuchâtel

where f is the electromagnetic wave frequency, and E(f) and H(f) are the Fourier spectra of the electric and magnetic fields.

A suitable horizontally-layered geological structure is then sought, the computed response of which gives the best possible fit of the observed set of $\varrho(f)$ data. It is generally assumed that this model gives a good picture of the vertical resistivity distribution.

Audio magnetotellurics

For natural frequencies above 1 Hz the method is called "audio magnetotellurics" (AMT). The sounding depth is limited by the penetration depth δ of the wave into the ground, seen as a conductor:

$$\delta \cong 503 \sqrt{\frac{\varrho}{f}} \text{ meters}, \tag{2}$$

with ϱ the resistivity in Ωm and f the frequency in Hertz, i.e. about 5000 meters at f = 1 Hz for homogeneous underground of 100 Ωm resistivity. The AMT method also uses natural electromagnetic fields which are present on the site. However, in most European regions and industrialized countries, the proliferation of man-made electromagnetic perturbations is rendering AMT soundings less and less feasible close to towns and villages.

The place of controlled-source AMT

Generally, electromagnetic fields of cultural origin cannot be used as signal sources, because they are often too close to the sounding site. The plane-wave condition required for using Rel. (1) is not fulfilled. Furthermore, source localization is difficult and the position generally varies with time.

These issues led Goldstein & Strangway (1975) to consider the use of a controlled source built around a power generator connected to the Earth through 2 electrodes (CSAMT method). Because the source can be controlled, it becomes possible to use synchronous detection techniques (lock-in) (Otten & Musmann 1982) or coherent signal stacking in order to extract geological information from the noise, or from signals that are not synchronized with the measurement.

In order to get more precise information on the structure of sedimentary basins, even in precarious conditions with strong man-made perturbations, we developed (Schnegg & Fischer 1984, Fischer & Schnegg 1986), and improved (Schnegg & Fischer 1988) a CSAMT sounding technique whose main caracteristics is that it can be deployed quickly.

2. Some aspects of the sounding method

The sounding equipment is made up of 2 parts:

1) the dipole source,
2) the receiving equipment.

2.1 Dipole source

The electric and magnetic signal amplitudes, as recorded by the receiver some hundred meters to some kilometers away from the source, are proportional to the source dipole strength, i.e., to the intensity of the current fed into the injection cable and to the dipole length. Source distance and azimuth are very sensitive parameters of the field so that the dipole length cannot be increased beyond a certain limit, if the point dipole approximation is to remain valid. We shall admit that the effective dipole length can reach half the source-receiver distance. It is always possible to approximate such a long dipole with a line of point dipoles, but at the price of extended computational effort.

The electric current that can be fed into the Earth is essentially limited by the finite electrical conductance of the ground. For example, in the rather favorable case of soil showing 500 Ω resistance between the electrodes, a sine or square wave source of 500 Volt can only supply 1 Ampere.

The problem of the contact resistance between the electrodes and the ground requires the sounding crew to devote several hours to fitting out the injection site in order to insure a sufficiently good electric contact. Several two-meter long steel stakes are generally used, and they take a considerable amount of time to drive into the ground. That was the motivation for developing a faster technique.

Our method makes use of 2 short electrodes (30 cm long, 3 cm diameter), easily driven into the ground. A 220 V, 2 kW gasoline generator, coupled to a high-voltage DC power supply, charges a 50 μF condenser bank up to 10 kV. A quartz clock monitored by timing signals from a regular transmitter insures synchronization at a rate of one pulse every 5 seconds. All the energy stored in the condenser bank is instantaneously released into the ground through a spark gap triggered by the timing pulse. With this technique, power peaks as high as 100 kW are available, with a fast rise-time. The advantages of this method are that a current of 10 A can be made to flow in spite of the use of rather primitive injection electrodes with contact resistance somewhat larger than that of long steel electrodes. The mean power over one cycle is 0.5 kW.

2.2 Receiving equipment

The receiving equipment does not differ much from AMT equipment. But since we intend to use our method in areas with little lateral inhomogeneity (tensor CSAMT modelling would be much harder), it is not necessary to measure both electric and magnetic field polarizations. We can therefore limit ourselves to sampling the electric field component parallel to the dipole source and the component of the magnetic field at a right angle. In actual fact, the electric field is measured simultaneously at 7 sites along the 500 m profile. Electrodes are placed every 70 meters. One measurement of the magnetic field in the middle of the line is sufficient, since this field is quite insensitive to the nature of the ground and does not vary much laterally. A 500-meter profile can therefore be sounded at one time [Fig. 1].

The receiver aperture is monitored by a second externally synchronized clock, insuring an absolute stability of a few micro seconds. In order to record the entire signal pulse, the source clock is intentionally delayed by a fixed time interval of 25 ms. After 15 minutes of data acquisition the signals of about 200 charge-discharge cycles will have

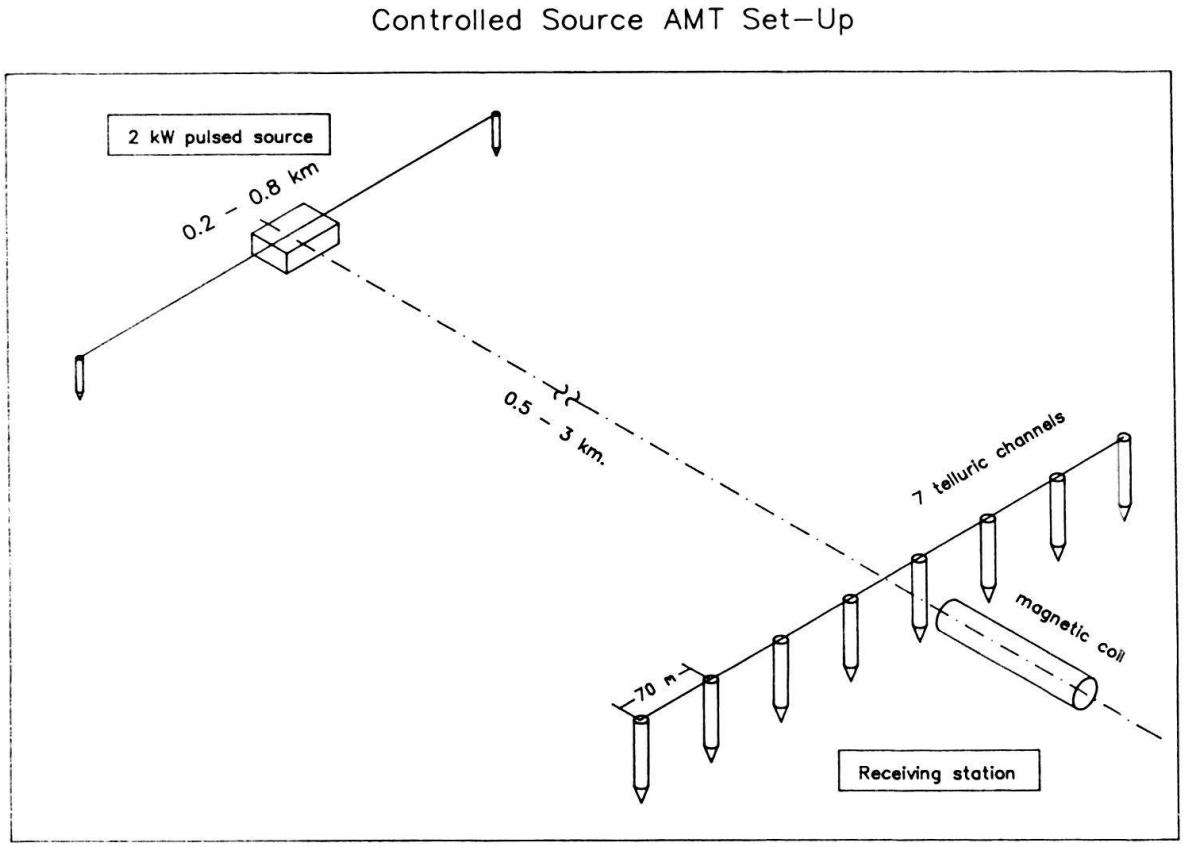

Fig. 1. Scalar CSAMT set-up. One sounding, including set-up and dismantling, can be achieved in 2 hours by a crew of 3.

been stacked. Signal addition is coherent, whereas noise is not, so that signal-to-noise ratio increases as $\sqrt{N}$, with N the number of discharges [Fig. 2].

When the signals are heavily contaminated by industrial fields ($16\frac{2}{3}$, 50 Hz), both clocks can be delayed by identical pseudo randomly-varying time intervals read from a ROM solid-state memory. When this is done, the perturbations synchronous with the mains look random from the CSAMT receiver side, and thus quickly vanish.

The projection of the borehole site on the electric field line is 120 meters away from the first electrode and the lateral distance is 130 meters.

3. The test site

The borehole TSCHUGG 1 (Swiss nat. coord. 572.610/207.910) was selected as the test site for evaluating our CSAMT method. Geological interpretation can be found in Schlanke et al. (1978). Located inside but close to the NW border of the Swiss Molasse Basin, between the lakes of Neuchâtel and Biel, the borehole shows the Lower Fresh-Water Molasse (Aquitanian and Chattian) beneath a 5-meter covering of Quaternary. Cretaceous limestones are found at 509 meters. The hole was drilled to a depth of 704 meters.

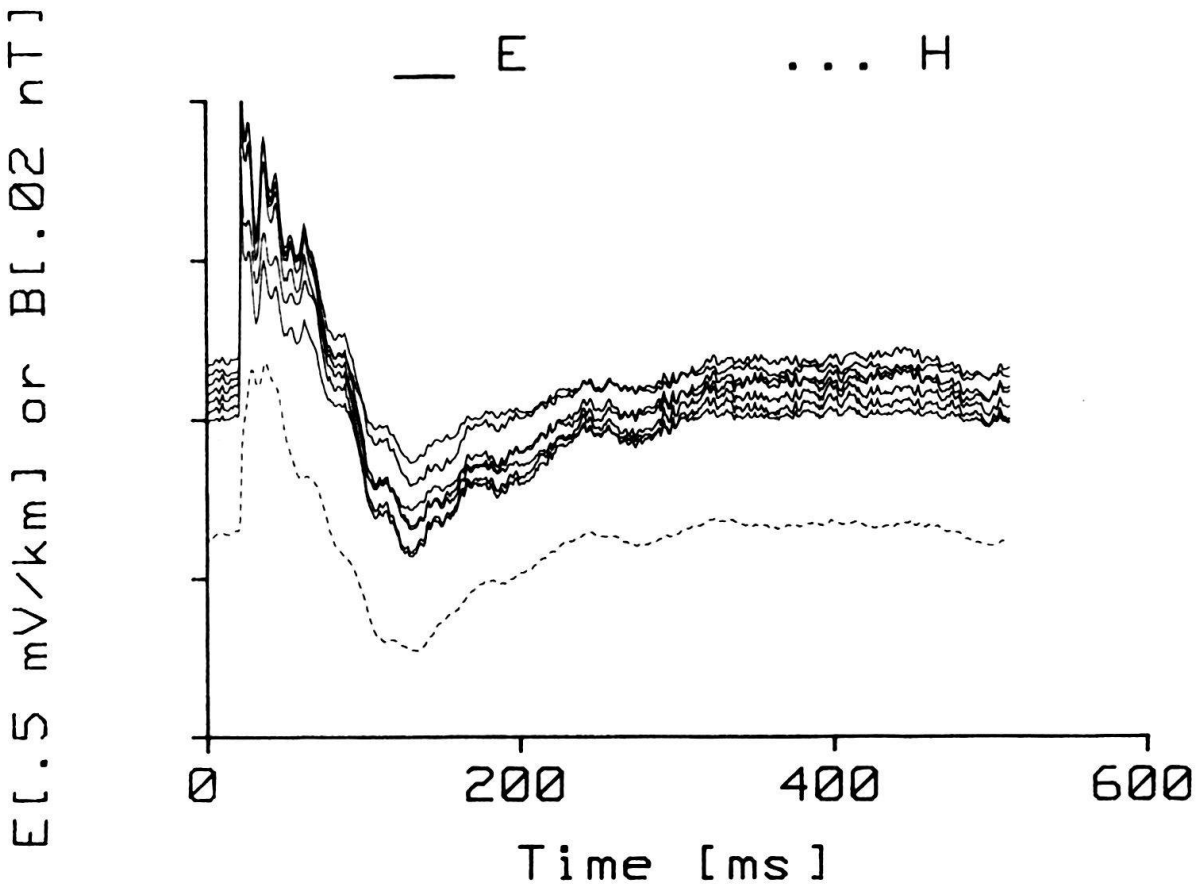

Fig. 2. Oscilloscope picture of recorded signals. Each signal is a coherent sum over 200 pulses, permitting a $\sqrt{200}$-fold increase in the signal-to-noise ratio. To avoid confusion the various tracks are plotted with different offsets. Note the presence of coherent noise visible before the pulse.

The electric resistivity log of the borehole was made available to us. The measured values have been smoothed by integrating the conductivity over 25-meter-thick slices. The result is shown in Fig. 3.

The resistivity of the Molasse decreases with depth, going through 3 successive steps of 30, 20 and 10 Ωm. The roof of the much more resistive Cretaceous is found at a depth of 509 m.

The telluric electrode line was deployed perpendicularly to the regional folding axis of the neighboring range, the Jura Mountains.

The current injection dipole ran parallel to the telluric electrode line. Two source distances were used: 2000 and 550 meters. The corresponding source dipole lengths were 700 and 200 meters (Fig. 1). The second source distance (550 m) was chosen to demonstrate that the resolving power of layer parameters becomes inadequate if the source distance is too short. The following results refer to the first source distance (2000 m).

4. Sounding results and comparisons

Fig. 4 shows the apparent resistivity and phase[2]) for the 7 telluric channels, as well as the response of the best 1-D models found through data modelling.

[2]) Note that our phase is 45° minus the phase of the MT impedance tensor.

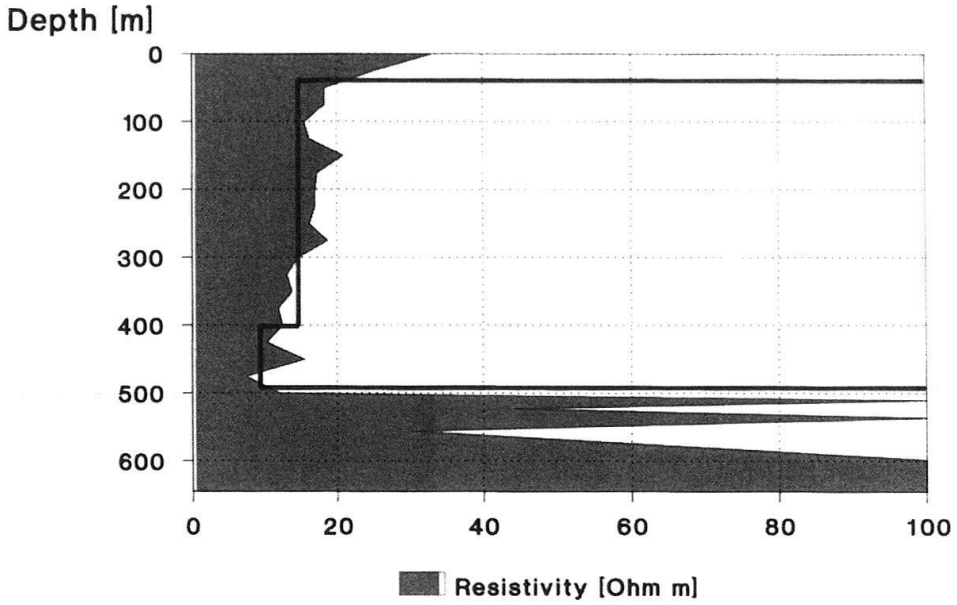

Fig. 3. Vertical electric resistivity distribution in the borehole as derived from the electric log (shaded area). The thick line gives the CSAMT model response.

Apparent resistivity and phase are computed the same way as for ordinary MT in the scalar case, where the telluric field in one direction is related only to the magnetic field at right angles (Eq. 1). In our CSAMT method the E(t) and H(t) signals originate from a coherent sum over about 200 pulses. The spectral power is mainly distributed over the frequency band under investigation: 1 Hz to 10 kHz. However, the higher part of this band (1 to 10 kHz) has to be measured separately, with a source distance of less than 200 meters, because the skin depth (Eq. 2) obviously also limits the horizontal wave propagation. For this frequency range, the injection dipole length is shortened accordingly. The configuration of the transmitter/receiver pair is no longer 100% broadside, but becomes a mixture of broadside and collinear geometries and the modelling program has to take this into account.

The apparent resistivity and phase modelling uses an optimizing algorithm (Beiner 1970) that looks for a vector

$$\{x_1^0, x_2^0, \ldots, x_N^0\}$$

which minimizes the function

$$\mathfrak{F}(x_1, x_2, \ldots, x_N). \tag{3}$$

In our case, the x_i are the resistivities and thicknesses of the N layers of a 1-D model. The function $\mathfrak{F}$ is the standard error of the model response compared with the measured values of the resistivity and (/or) the phase. This response is computed in a subroutine giving the electric and magnetic fields at the surface of horizontal stratification as a function of the layer resistivities and thicknesses, of the distance and of the frequency of an electric dipole (Weidelt 1984).

The search for the best model is done independently for each of the 7 sites. Since lateral variations of resistivity are in effect small (we assume a quasi horizontal layering;

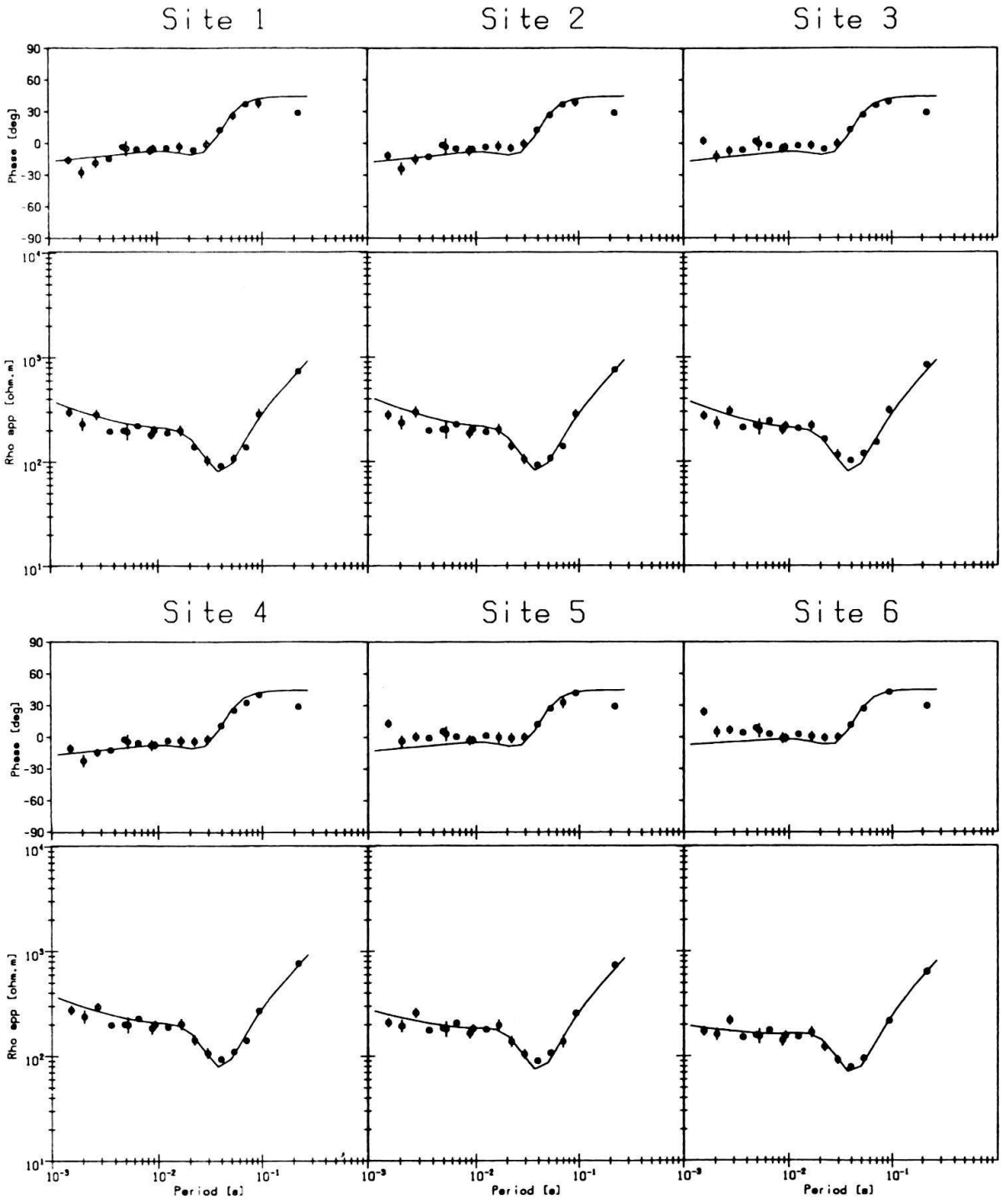

Fig. 4. CSAMT data for six telluric channels located along the 500 m profile. Both the apparent resistivity and the phase have been modelled. The solid lines give the responses of the best-fitting models.

this condition is likely to occur (Axelrod 1978) within a circle of 10 km radius), the final model for one site is used as starting model for the next site. Resistivity variations between two sites are generally smaller than 10% and should be considered as non-representative of the nature of the underground. The same is true for the computed layer thicknesses whose large scatter is mainly caused by data noise. In order to avoid prop-

agating the resistivity instabilities to the layer thicknesses, we modelled the 7 sites again, giving each layer a fixed resistivity corresponding to the mean resistivity over that layer for the 7 sites. Thus, only each layer thickness was allowed to adapt freely. Fig. 5 shows the seven models obtained.

The same number of layers was chosen for each site (5 layers). This number was selected because one more layer did not lead to a significant decrease of the modelling error $\mathfrak{F}$ defined in Eq. 3 (Fischer & Le Quang 1982).

The model obtained for site 1, the site nearest to the borehole (177 m) is seen in Fig. 3, where it is compared with the results of the smoothed borehole resistivity log. It can be seen at once that the depth to the Molasse-Mesozoic interface is obtained with great accuracy (491 m instead of 509 m). The same is true for the resistivity values found for the Molasse. In situ measurement reveals 3 domains of somewhat distinct mean resistivity (22, 17 and 12 Ωm) with interfaces at about 50 and 300 meters. Our CSAMT sounding also shows 3 domains (170, 14 and 8 Ωm) with interfaces at 37 and 402 meters. The discrepancy observed for the resistivity of the upper layer is due to a low signal to noise ratio at the high frequency end of the sounding curves, with the rho curves biased upwards by cultural electric noise. With a closer source (at 550 m, Fig. 8) the error diminishes.

The resistivity obtained for the Cretaceous limestones is larger than the reference value (1 000 Ωm against 50–200 Ωm). For the purpose of modelling it appears that the resistivity of a low-conductivity layer is a rather insensitive parameter. Even large variations of such a parameter do not have much effect on the error $\mathfrak{F}$.

Accuracy of direct measurement of the resistivity of low-conductivity rocks in the borehole is also questionable because it can be spoilt by water contamination.

Fig. 6 shows the trade-off diagram (Fischer & Le Quang 1982) for every model parameter (resistivities ϱ_i and thicknesses h_i), i.e., the factor by which the parameter can be multiplied (or divided) to increase the error $\mathfrak{F}$ by at most 10%. It can be seen that

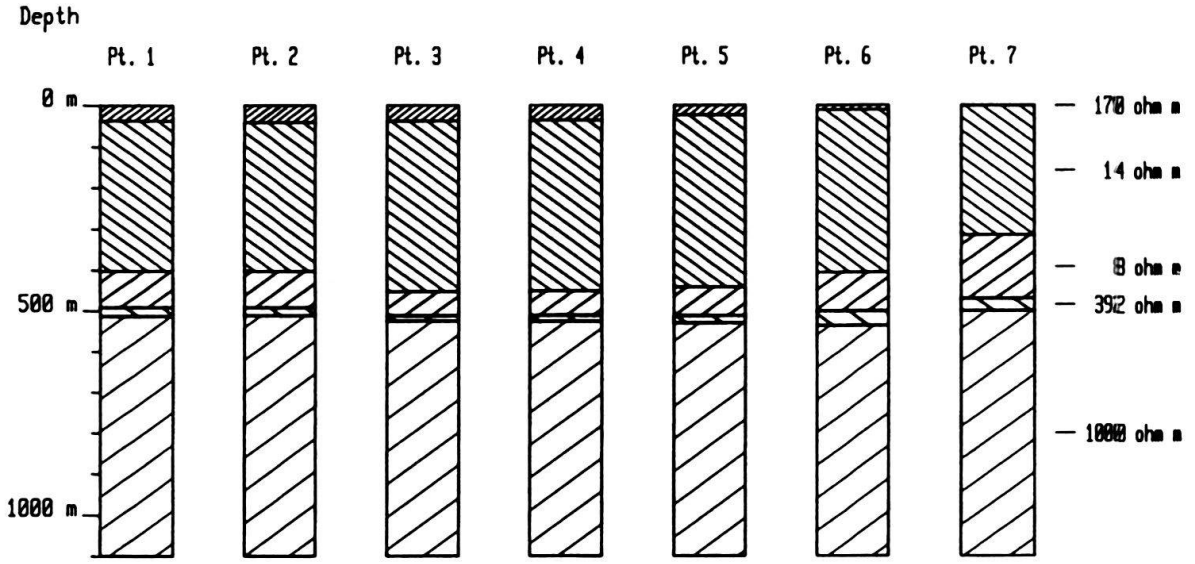

Fig. 5. Corresponding 1-D models for the seven telluric channels. The modelling was done in two phases: 1) determination of mean resistivity values over the 7 channels for each layer (these values are given on the right-hand side of the figure); 2) modelling of the layer thicknesses, keeping the resistivities constant.

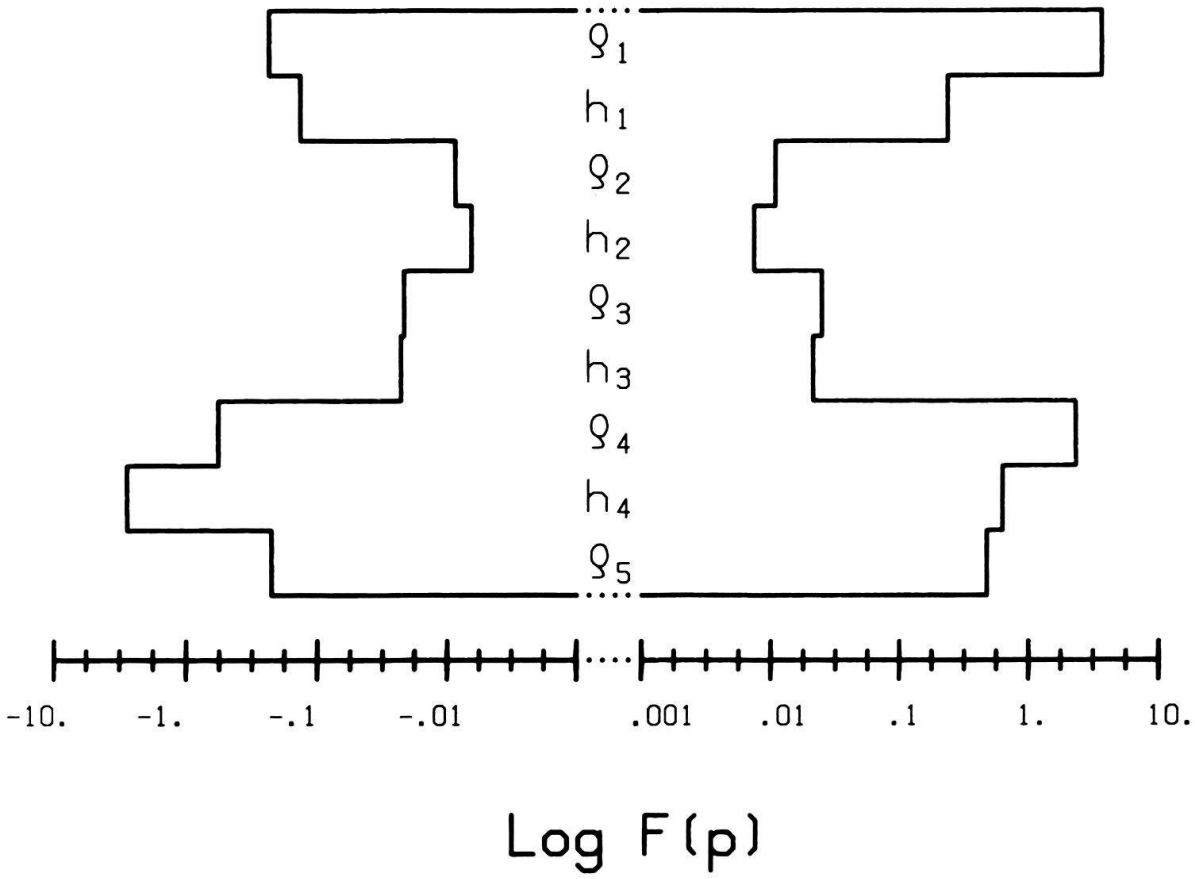

Fig. 6. Parameter sensitivity diagram. The boundaries of the abscissa give the logarithms of the numbers F(p) by which a parameter can be multiplied (right) or divided (left) while keeping the misfit within 10% of its minimum value. Note that the scale is double logarithmic.

layers 2 and 3 are tightly constrained (1 to 4%). This is not true for layers 1,4 and 5, which are much more resistive layers.

5. Comparison with audio magnetotellurics

For the purpose of comparison an AMT sounding was carried out at site 1, close to the borehole. Fig. 7 shows the results of this sounding in both measurement axes. In Polarization 1, the telluric line has the same direction as the CSAMT electric line, i.e. perpendicular to the folding axis of the Jura range.

The apparent resistivity data display two foreseeable biases:

I. At periods above 0.01 s an increase of the apparent resistivity with a slope close to 45°. The effect is particularly evident in Pol. 1, and can be understood by the influence of a neighboring artificial signal source, namely a DC railway line 2 km away. As predicted by the dipole field theory, collinear geometry of Pol. 1 produces apparent resistivity curves with slopes larger than that of broadside geometries (Pol. 2).

One-dimensional modelling of these data is shown on Fig. 8. Notice that the influence of this type of perturbation is a strong exaggeration of the resistivity of deeper layers: the model displays a value of 64 Ωm instead of an effective 10–20 Ωm.

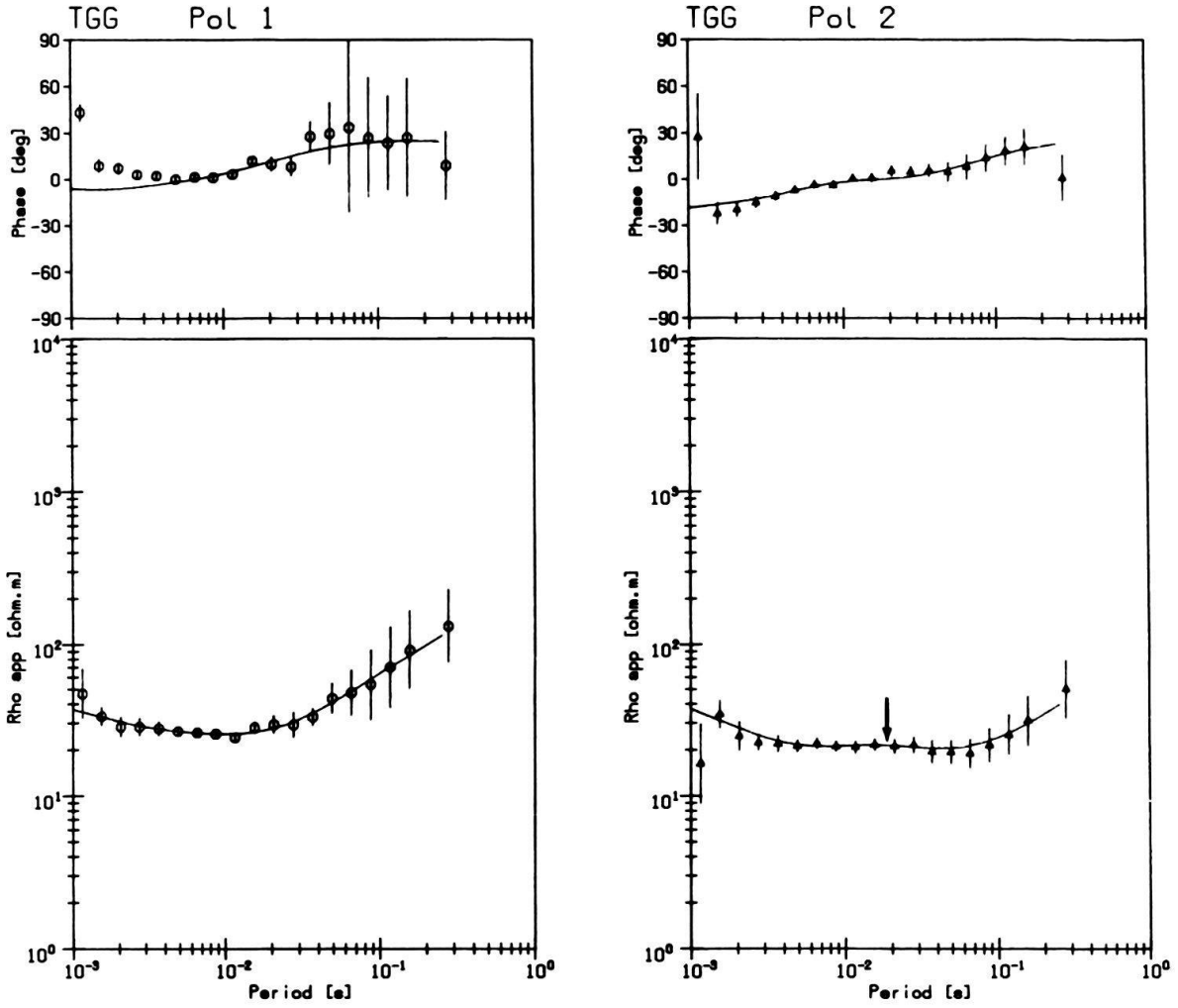

Fig. 7. AMT data measured near the borehole. The influence of current leakage from a nearby DC railway is seen in Pol. 1 as an anomalous slope of apparent resistivity. AC power at $16\frac{2}{3}$ Hz produces a bump (arrow) visible in the apparent resistivity of the Pol. 2 data. The solid lines are the responses of the best-fitting models shown in Fig. 8.

II. The presence of a bump between 16 and 100 Hz, to be seen on both polarizations. Here, it is a residual $16\frac{2}{3}$ Hz artificial signal and its harmonics (AC trains) that produces this slight bend on the apparent resistivity curves. In Pol. 2 this perturbation simulates the presence of a highly resistive layer ($> 10^5$ Ωm) of 100 m thickness. In Pol. 1 this effect is masked by effect I. Note here that the pronounced minimum of the measured apparent resistivity curves of Fig. 4, occurring in this frequency band, is typical of CSAMT and is not a noise artifact.

Fig. 8 also shows the CSAMT model obtained when the signal source is closer to the sounding site (here: 550 meters). The main characteristics are kept, but much of the structural accuracy is lost. This shows the importance of finding a good trade-off between source distance and signal strength. Signal quality and its content in meaningful geological information must be considered simultaneously.

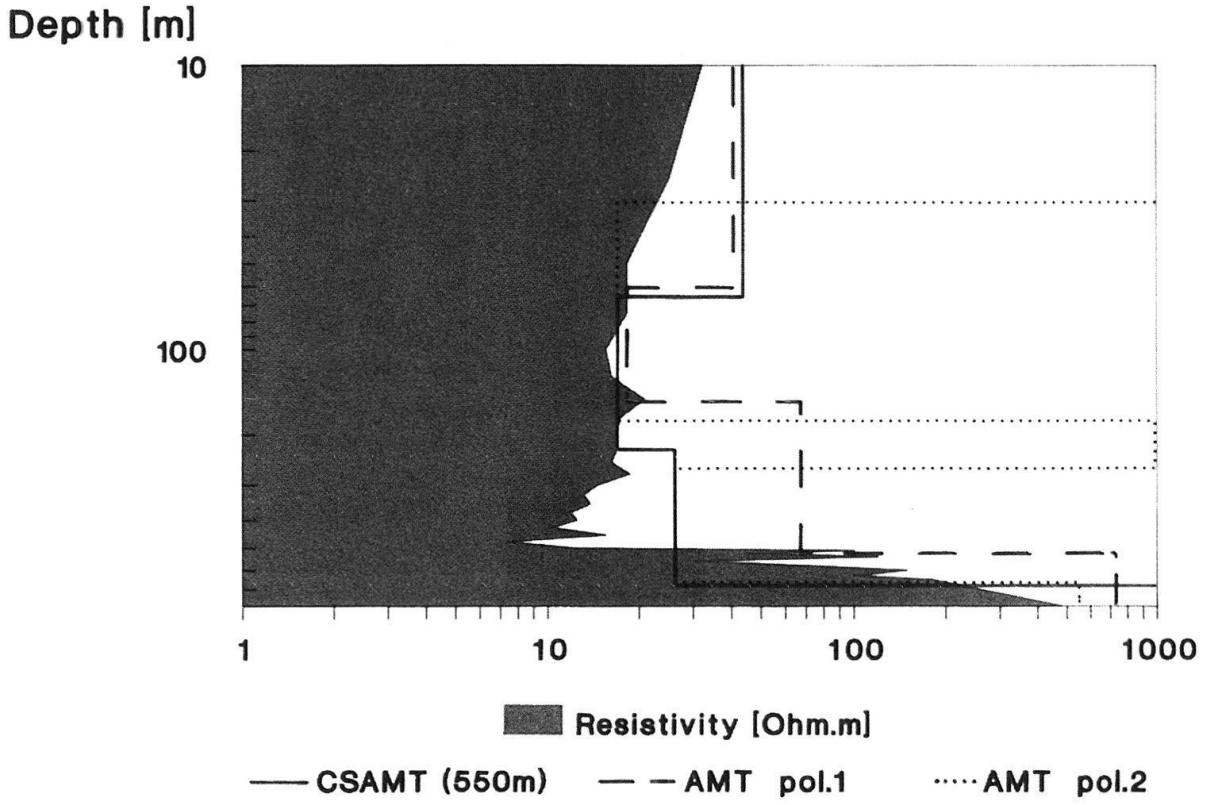

Fig. 8. Comparison of three models with the actual geology. The solid line shows the best CSAMT model found when the source is too close. The two broken lines correspond to AMT models. An erroneous 4th layer in Pol. 1 and an extra layer in Pol. 2 originate from the biases described in Fig. 7.

6. Comparison with the Schlumberger geoelectric sounding

A few years ago two Schlumberger soundings were carried out within 2 km of our test side (Axelrod 1978), with distances O A of 300 and 400 m. The information secured by this technique did not extend deeper than 50 m and revealed a 4 m-thick Quaternary layer over 25 to 31 Ωm material.

7. Conclusions

The CSAMT method possesses a remarkable resolving power in the study of quasi-horizontally layered formations. By means of a relatively light instrument, the method is capable of localizing well-contrasted interfaces with an error of only a few percent. Its superiority over the AMT method rests on its immunity to external perturbing effects.

The comparison with the Schlumberger geoelectric sounding method is very advantageous for CSAMT. For an equivalent amount of work (mainly the laying-out of electric lines), an investigation depth 5 to 10 times greater is obtained.

However, as is the case for Schlumberger soundings, CSAMT is rather sensitive to lateral variations of the resistivity. Consequently, it is of upmost importance to choose the sounding sites correctly if all the intrinsic advantages of the method are to be exploited.

Acknowledgments

The author is grateful to Dr. L. Hauber, chief geologist of the Canton of Basel for providing access to the TSCHUGG 1 electric log.

Financial assistance from the Swiss National Sciences Foundation and the Geophysical Commission of the Swiss Academy of Sciences is also acknowledged.

REFERENCES

AXELROD, A. 1978: Contribution à l'étude géophysique de la région des lacs de Neuchâtel, Bienne et Morat, doctoral thesis, Université de Lausanne.

BEINER, J. 1970: FORTRAN routine MINDEF for function minimization, Institut de Physique, Université de Neuchâtel.

CAGNIARD, L. 1953: Basic Theory of the Magneto-Telluric Method of Geophysical Prospecting. Geophysics 18, 605–635.

FISCHER, G. & LE QUANG, B. V. 1982: Parameter Trade-off in One-Dimensional Magnetotelluric Modelling, J. Geophys. 51, 206–215.

FISCHER, G. & SCHNEGG, P.-A. 1986: Modelling Active Audio Magnetotelluric Data. J. Geophys. 59, 49–55.

GOLDSTEIN, A. & STRANGWAY, D. W. 1975: Audio-frequency Magnetotellurics with a Grounded Electric Dipole Source. Geophysics 40, 669–683.

KELLER, G. V. & FRISCHKNECHT, F. C. 1979: Electrical Methods in Geophysical Prospecting. International Series in Electromagnetic Waves 10, Pergamon Press.

OTTEN, J. & MUSMANN, G. 1982: Aktive Audiomagnetotellurik bei Travale. Protokoll Elektromagnetische Tiefenforschung, Neustadt a. W. 183–188.

SCHLANKE, S., HAUBER, L. & BÜCHI, V. P. 1978: Lithostratigraphie und Sedimentpetrographie der Molasse in den Bohrungen Tschugg I und Ruppoldsried I (Berner Seeland), Eclogae geol. Helv. 71, 409–425.

SCHNEGG, P.-A. & FISCHER, G. 1984: A New Pulsed Audio Magnetotelluric Technique. J. Geophys. 55, 191–198.

– 1988: A Multichannel CSAMT Technique. Proc. of the 9th Workshop on Electromagnetic Induction in the Earth and Moon, IAGA Working Group 1–3, Sochi, USSR (1988).

SZARKA, L. 1987: Geophysical Aspects of Man-Made Electromagnetic Noise in the Earth – A Review. Surveys in Geophysics 9, 287–318.

TIKHONOV, A. N. 1950: On Determining Electrical Characteristics of the Deep Layers of the Earth's Crust. Dokl. Akad. Nauk. SSSR 73, 295–297 [in Russian].

WEIDELT, P. 1984: FORTRAN routine BIPOL for the computation of dipole fields, Technische Universität Braunschweig.

Manuscript received 18 November 1991
Revision accepted 9 March 1992